EXPERIMENTAL STUDY ON THRESHING POWER CONSUMPTION OF AN AXIAL-FLOW THRESHING DEVICE WITH ADJUSTABLE THRESHING INTENSITY
/
脱粒力度可调式轴流脱粒装置脱粒功耗试验研究

Yuejiang TENG[1,2], Chengqian JIN[*3], Fuxiang XIE[1,2], Jian SONG[1,2]
[1] School of Machinery and Power Engineering, Weifang University, Weifang / China;
[2] Shandong Key Laboratory of Intelligent Manufacturing Technology for Advanced Power Equipment, Weifang / China;
[3] Nanjing Institute of Agricultural Mechanization, Ministry of Agriculture and Rural Affairs, Nanjing / China
Tel: +86-19525369138; E-mail: tyj2021to2026@163.com
Correspondent author: Chengqian JIN
DOI: https://doi.org/10.35633/inmateh-79-34

Keywords: *axial-flow threshing device, adjustable threshing intensity, threshing power consumption, mechanical efficiency, parameter optimization*

ABSTRACT
To address the high power consumption, limited load adaptability, and inadequate parameter matching of conventional axial-flow threshing devices, power-consumption tests were conducted on an axial-flow threshing device with adjustable threshing intensity using rice as the test material. The tests examined different threshing-intensity modes, separating-screen types, and operating parameters. The effects of these factors on no-load power consumption, effective power consumption, total power consumption, and mechanical efficiency were analyzed. The results showed that total power consumption was minimized when the threshing-intensity adjustment plates were fully open and the rectangular-hole separating screen was used. Total power consumption increased with increasing drum speed, deflector angle, and feed rate, but decreased with increasing concave clearance. Mechanical efficiency initially remained stable and then decreased as drum speed increased, whereas it increased with increasing deflector angle and feed rate. The specific threshing power consumption, expressed per unit feed rate, ranged from 4.4 to 5.2 kW/(kg/s). It increased with increasing drum speed, deflector angle, and feed rate, and decreased with increasing concave clearance. This study provides a reference for reducing power consumption and optimizing parameter matching in axial-flow threshing devices with adjustable threshing intensity.

摘要
针对传统轴流脱粒装置功耗偏高、负荷适应性差、参数匹配粗放等问题，以水稻为试验材料，在一种脱粒力度可调式轴流脱粒装置上，开展不同脱粒力度模式、分离筛板类型及不同工作参数条件下的脱粒功耗试验，分析各试验因素对空载功耗、有效功耗、总功耗及机械效率的影响规律。结果表明：脱粒力度调节板全部打开、采用长方形筛孔式分离筛板时总功耗最低；总功耗随滚筒转速、导流板角度、喂入量的增大而上升，随凹板筛间隙的增大而下降；机械效率随转速的升高先稳后降，随导流板角度及喂入量的增大而提高。装置单位喂入量脱粒功耗为 4.4～5.2 kW/(kg/s)，随滚筒转速、导流板角度、喂入速率的增加而升高，随凹板筛间隙的增大而降低。该研究可为脱粒力度可调式轴流脱粒装置低功耗优化与参数匹配提供参考。

INTRODUCTION
As the core working component of a grain combine harvester, the threshing device accounts for the highest proportion of the total power consumption of the whole machine. The characteristics of threshing power consumption directly affect the power matching, operating efficiency and performance, as well as fuel economy of the combine harvester *(Song et al., 2022; Li et al., 2011; Mousaviraad et al., 2020)*. In practical harvesting operations, operating parameters such as drum speed, concave clearance and feed rate jointly determine the threshing power consumption and the mechanical efficiency of the device *(Kiniulis et al. 2017; Qin et al., 2025; Yu et al., 2025)*. At present, harvesting equipment generally suffers from problems such as extensive parameter matching, high operating power consumption, large fluctuations in mechanical efficiency and poor load adaptability *(Lu et al., 2012; Chen et al., 2025; Vlăduț et al., 2022)*.

Yuejiang Teng, Lecturer, Ph.D.; Chengqian Jin, Prof., Ph.D.; Fuxiang Xie, Prof., Ph.D.; Jian Song, Prof., Ph.D.

Especially under complex field conditions with uneven feeding and drastic changes in crop moisture content, problems such as blockage, sharp increase in energy consumption, incomplete threshing or excessive grain damage frequently occur, which seriously restrict the upgrading and development of combine harvesters toward high efficiency, low consumption, intelligence and lightweight *(Jin et al., 2015; Ren et al., 2013; Steponavičius et al. 2023; Vlăduţ et al., 2023; Zhang et al., 2026)*.

In recent years, scholars worldwide have conducted extensive research on the structural optimization, parameter matching, and power consumption characteristics of axial-flow threshing devices. *Waree et al. (2016)* investigated the effects of structural parameters on the power consumption of an axial-flow corn threshing device using the response surface methodology. The results indicated that increasing the tine clearance, concave grate clearance, and concave clearance could significantly reduce threshing power consumption. Meanwhile, a power consumption prediction model with high fitting accuracy was established, which provided a theoretical basis for the low-energy structural parameter optimization of threshing devices. *Fan et al. (2022)* developed an adaptive feed-rate threshing clearance control system to address the excessive power consumption caused by non-adjustable threshing clearance under varying feed rates. Tests showed that the system could match the optimal threshing clearance, with the average power consumption increased by only 3.45%. The system significantly improved operating performance while maintaining basically stable energy consumption, providing a feasible approach for the energy-saving control of threshing devices. *Ali et al. (2024)* optimized the rotor structure of sunflower threshers to conduct experiments for energy consumption reduction. Their test results verified that rotor rotary speed and concave clearance exert remarkable impacts on the specific energy consumption during threshing operations. When adopting the tine-bar rotor under the working condition of 300 r/min rotor speed and 10 mm concave clearance, the specific energy consumption was reduced from 9.65 kWh/ton to 5.09 kWh/ton. This finding demonstrated that structural improvement of threshing rotors was an effective method to reduce the power consumption of threshing operations. *Xing et al. (2024)* designed a longitudinal-axial flow threshing device with a measurement and control system to tackle the high energy consumption and poor parameter matching of corn ear threshing under high moisture content. Parameter optimization tests were carried out with drum speed, concave clearance, and deflector angle as variables. A regression model of unit energy consumption was established and the optimal parameters were obtained. Results showed that the unit energy consumption was reduced by 14.74% after optimization with high model accuracy, offering a reference for the low-power consumption optimization of threshing devices.

Most existing studies focused on threshing devices with fixed structures and single adjustment mode, and there is a lack of research on the power consumption characteristics of novel axial-flow threshing devices with adjustable threshing intensity, multi-mode switching and multi-parameter collaborative regulation *(Wang et al., 2025; Xie et al., 2021)*. In particular, studies on the variation laws of power consumption and mechanical efficiency under the coupling effects of different threshing intensity modes, separating screen types, concave clearance, deflector angle and other parameters are insufficient.

Therefore, this study took an axial-flow threshing device with adjustable threshing intensity as the research object. The device integrated an adjustable-intensity threshing concave, a 360° separation device, a concave clearance adjustment mechanism, and a deflector angle adjustment mechanism, which could realize the switching of four threshing intensity modes and multi-parameter collaborative regulation. Threshing power consumption tests were carried out under different threshing intensity modes, separating screen types, drum speeds, deflector angles, concave clearances and feed rates. The variation laws of no-load power consumption, effective threshing power consumption, total threshing power consumption and mechanical efficiency were systematically analyzed, and the influence mechanism of each parameter on threshing power consumption was revealed. This study could provide experimental evidence and theoretical support for the low-energy optimization and parameter matching of adjustable axial-flow threshing devices

MATERIALS AND METHODS

Structure of the longitudinal-axial flow threshing device with adjustable threshing intensity

The threshing intensity required during harvesting varies considerably among crop varieties, moisture contents, and feed-rate conditions. The complexity of practical threshing conditions therefore imposes greater requirements on the adaptability of the threshing device. To address these requirements, a longitudinal axial-flow threshing device with adjustable threshing intensity was designed, as shown in Fig. 1. The device mainly consists of a screw feeder, a trapezoidal threshing drum, an adjustable-intensity threshing concave, a 360° separation device, concave-clearance adjustment mechanisms, deflectors, and a deflector-angle adjustment mechanism.

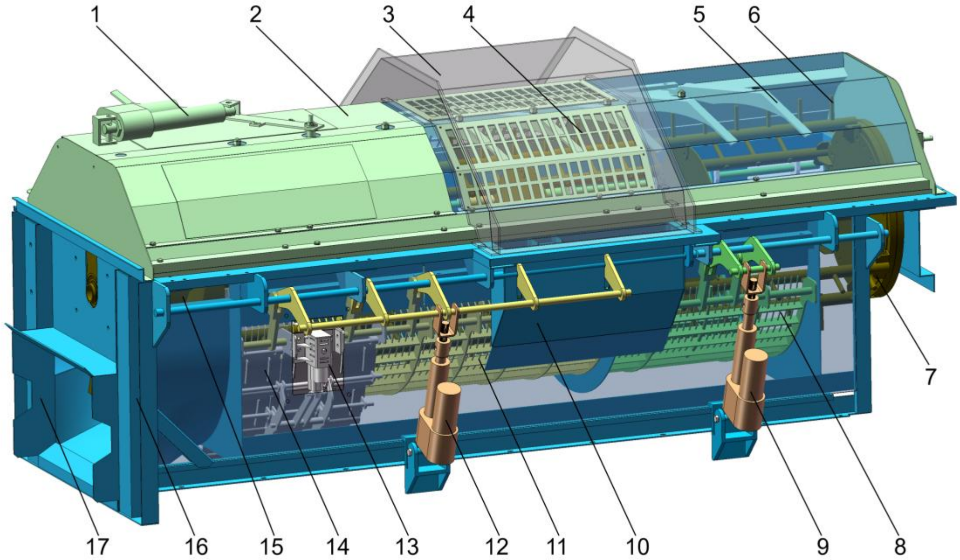

Fig. 1 - Structure of the longitudinal-axial flow threshing device with adjustable threshing intensity

1 – deflector angle adjustment mechanism; 2 – top cover; 3 – 360° separation device; 4 – upper sieve plate of 360° separation device; 5 – deflector; 6 – threshing element; 7 – trapezoidal threshing drum; 8 – separating concave; 9 – separating concave clearance adjustment mechanism; 10 – return plate of 360° separation device; 11 – threshing concave; 12 – threshing concave clearance adjustment mechanism; 13 – adjustable-intensity threshing concave; 14 – threshing-intensity adjustment plate; 15 – screw feeder;16 – frame; 17 – feed inlet

The structure of the adjustable-intensity threshing concave is shown in Fig. 2. It mainly consists of threshing intensity adjustment plates, transverse grids, concave bars, side arc plates, electric actuator mounts, electric actuators and transmission rods.

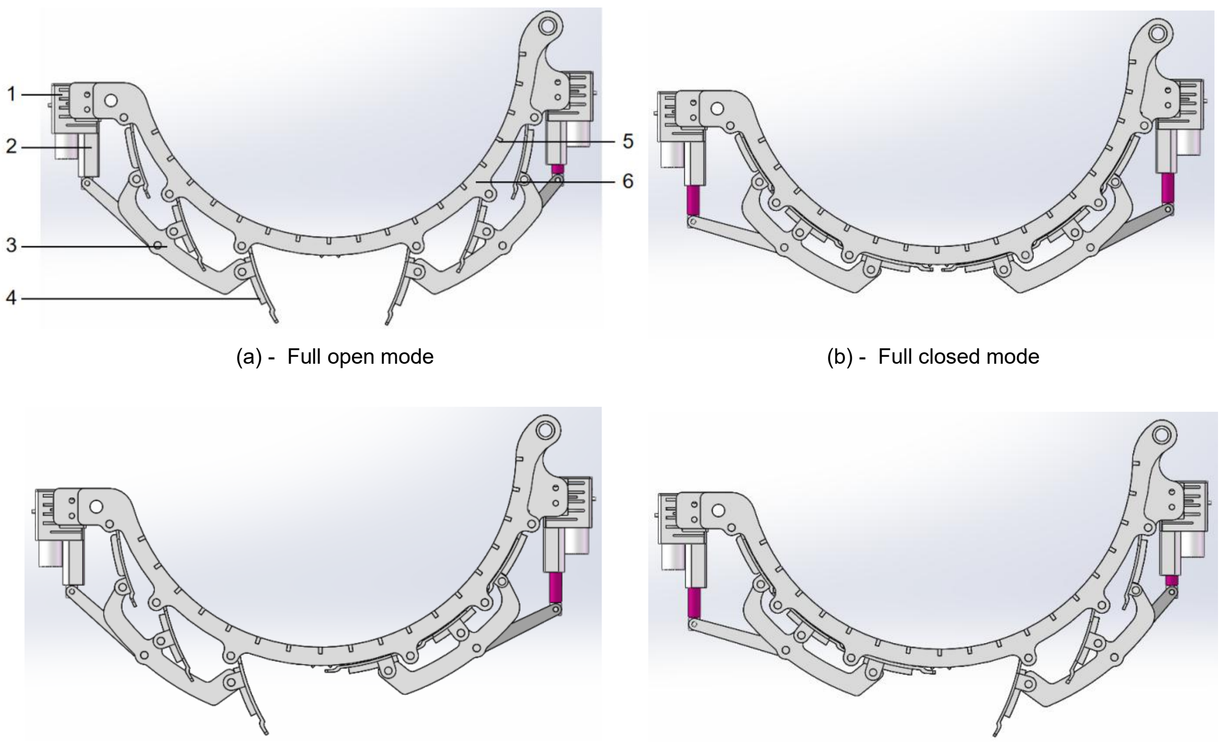

(a) - Full open mode (b) - Full closed mode

(c) - Left open and right closed mode (d) - Left closed and right open mode

Fig. 2 - Structure and operating modes of the adjustable-intensity threshing concave

1 – electric actuator mount; 2 – electric actuator; 3 – transmission rod; 4 – threshing-intensity adjustment plate; 5 – transverse partition plate; 6 – Side arc plate

The threshing-intensity adjustment plates were divided into left and right parts. Each part contained 9 adjustment plates arranged in 3 rows and 3 columns.

Each adjustment plate was hinged on one side to the concave frame, and the other side was uniformly controlled by an electric actuator through a transmission mechanism to switch between open and closed states. The left and right electric actuators were both fixed on the concave frame. According to the required threshing intensity during operation, the threshing-intensity adjustment plates could be adjusted to four modes: fully open, fully closed, left open and right closed (viewed from the rear of the threshing device), and left closed and right open (viewed from the rear of the threshing device), as shown in Fig. 2.

Test materials

Compared with other grains, rice grains and stems have higher moisture content, resulting in relatively high power consumption during threshing. Therefore, rice was selected as the test material in this study to investigate threshing power consumption. The relevant material properties of rice are listed in Table 1.

Table 1

Relevant material characteristic parameters of the test crop

Test crop	Plant height [mm]	Straw-to-grain ratio	Grain moisture content [%]	Stem moisture content [%]	Thousand-grain weight [g]	Yield per unit area [kg·hm^{-2}]
Rice	865	1:1.1	23.2	58.6	27.5	8960

Test Method

The power consumption of the threshing device measured in the experiment included no-load power consumption, effective threshing power consumption, and total threshing power consumption. No-load power consumption referred to the power required to maintain the rotation of the threshing drum. Effective threshing power consumption was the power consumed for crop threshing. Total threshing power consumption, which is the sum of no-load power consumption and effective threshing power consumption, represented the total power required for the threshing operation of the device. The power consumption of the threshing device *(Wan et al., 2005; Zhang et al., 2010)* was calculated using Equation (1).

$$P=\frac{Mn}{9550} \tag{1}$$

where: P is power consumption of the threshing device, kW; M is torque acting on the threshing drum during operation, N·m; n is rotational speed of the threshing drum, r/min.

The experimental measurement equipment included a wireless torque measuring device, a data receiving device, a drum rotational speed measuring device, etc., as shown in Fig. 3. Before the experiment, the strain gauges of the torque acquisition device were adhered to the ground surface of the main shaft of the threshing drum with glue and fixed with adhesive tape. The wireless torque node and battery were also fixed on the main shaft of the threshing drum with adhesive tape. During the test, the torque data acting on the drum was transmitted to a computer through a wireless gateway. An encoder was installed at the rear of the threshing drum and connected to the main shaft of the drum via a coupling. The real-time rotational speed of the threshing drum could be measured by the encoder when the threshing device was in operation. The threshing power consumption could be obtained by substituting the torque and rotational speed parameters into Equation (1).

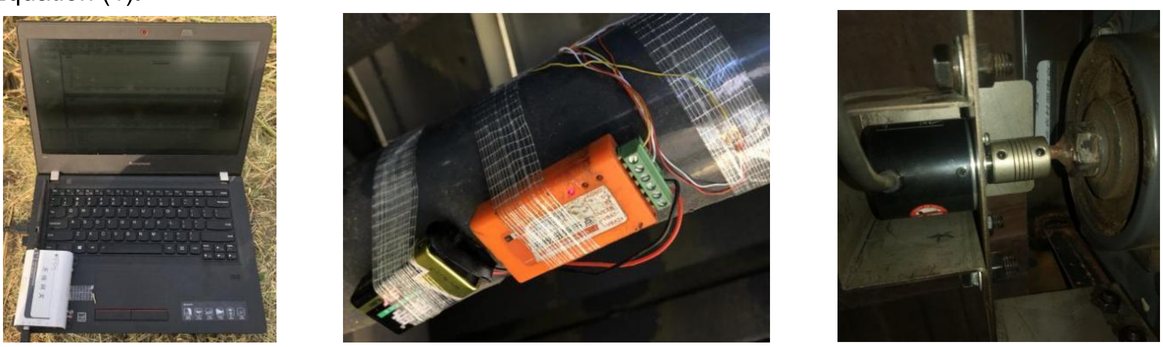

(a) - Data receiving and processing device (b) - Drum torque acquisition device (c) - Drum rotational speed measurement device

Fig. 3 - Equipment used to measure threshing power consumption

To investigate the influence laws of different structural parameters of the threshing device on its power consumption, comparative experiments were carried out on the threshing power consumption under different switching modes of the adjustable threshing force concave sieve (as shown in Fig. 2) and different types of separation sieve plates at the upper part of the 360°separation device (as shown in Fig. 4), respectively.

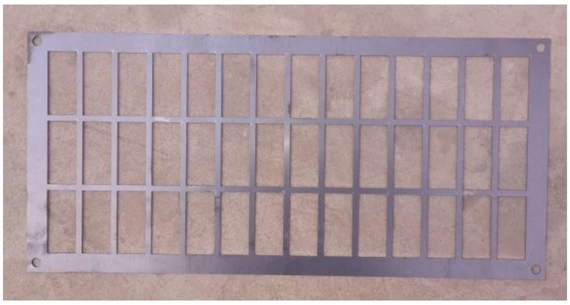

(a) - Rectangular-hole sieve plate

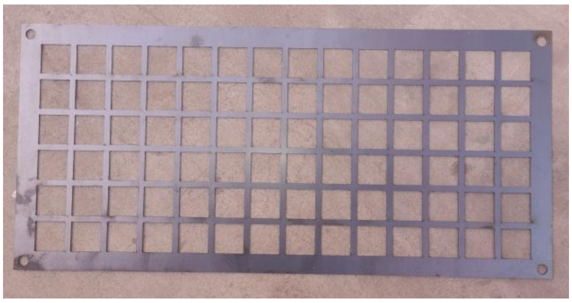

(b) - Square-hole sieve plate

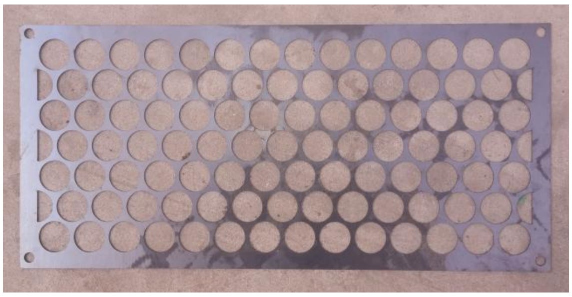

(c) - Circular-hole sieve plate

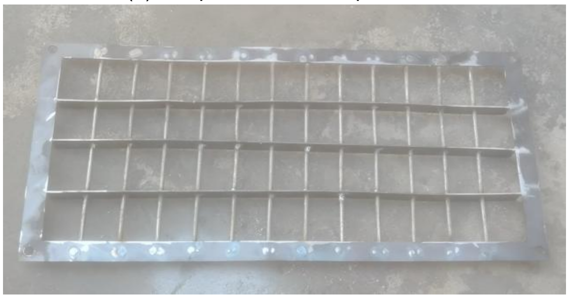

(d) - Grid-type sieve plate

Fig. 4 - Different types of sieve plates used in the upper separation device

The basic operating parameters of the threshing device were set as follows *(Jiang et al., 2025; Zhou et al., 2022; Liu et al., 2025)*: drum rotational speed of 900 r/min, deflector angle of 60°, concave sieve clearance of 20 mm, and Feed rate of 4 kg/s. In the comparative experiment of threshing power consumption under different switching modes of the adjustable threshing force concave sieve, the upper part of the 360° separation device was equipped with a rectangular-hole separation sieve plate. In the comparative experiment of threshing power consumption with different types of separation sieve plates for the 360° separation device, the threshing force adjustment plates were fully opened.

To investigate the influence law of operating parameters on the threshing power consumption of the threshing device, single-factor tests were conducted by selecting rotational speed of the threshing drum, deflector angle, concave sieve clearance and feed rate as influencing factors. During the experiments, the threshing force adjustment plates were fully opened, and the upper part of the 360° separation device was equipped with a rectangular-hole separation sieve plate. The adjustment method of the operating parameters is shown in Fig. 5. The level coding design of the experimental influencing factors is presented in Table 2.

(a) -Drum rotational speed adjustment device (b) - Deflector angle adjustment device (c) Concave sieve clearance adjustment device

Fig. 5 - Operating parameters adjustment devices

Table 2

Experimental factors coding

Coded Value	Drum rotational speed [r·min^{-1}]	Deflector angle [°]	Concave clearance [mm]	Feed rate [kg·s^{-1}]
-1	800	50	10	3
-0.5	850	55	15	3.5
0	900	60	20	4
0.5	950	65	25	4.5
1	1000	70	30	5

RESULTS AND DISCUSSION

The results of the comparative tests on threshing power consumption under the different operating modes of the adjustable-intensity threshing concave are shown in Fig. 6. Among the four modes, total threshing power consumption was lowest, at 27.14 kW, when the threshing-intensity adjustment plates were fully open, and highest, at 27.67 kW, when they were fully closed. When the adjustment plates were fully open, the effective separation area of the concave was larger, which reduced the amount of crop material retained in the threshing chamber and decreased threshing resistance. Consequently, total threshing power consumption was minimized. When viewed from the rear of the device toward the front, the threshing drum rotated counterclockwise. Under this direction of rotation, threshing resistance was lower in the left-open/right-closed mode than in the left-closed/right-open mode. Accordingly, the total threshing power consumption was lower in the left-open/right-closed mode.

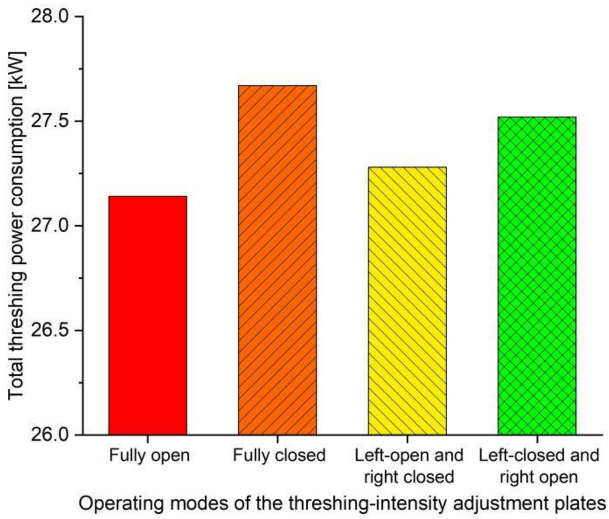

Fig. 6 - Comparison of total threshing power consumption among the operating modes of the threshing-intensity adjustment plates

The results of the comparative tests on threshing power consumption using different separation sieve plates in the 360° separation device are shown in Fig. 7.

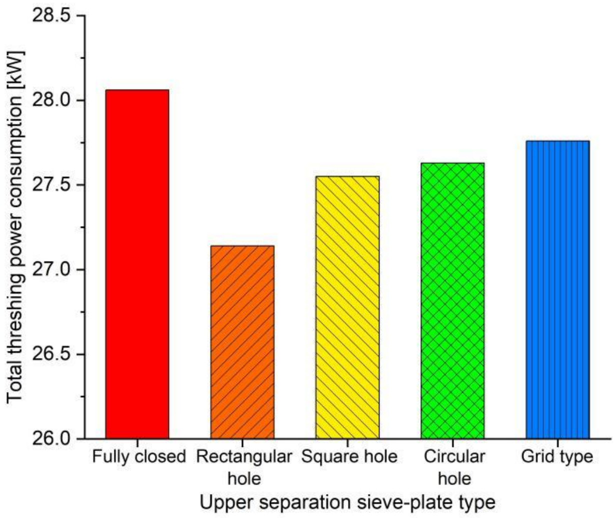

Fig. 7 - Comparison of total threshing power consumption among different upper separation sieve-plate types

As shown in Fig. 7, when the upper concave sieve of the 360° separation device was fully closed, the threshing power consumption was 28.06 kW, which was significantly higher than that under the open condition.

This phenomenon could be attributed to the reduced separation area of the concave sieve in the fully closed state, which prolonged the threshing and separation duration of crops in the threshing chamber and thus increases the threshing power consumption of the drum. The order of threshing power consumption for different types of separation sieve plates from low to high was as follows: rectangular-hole sieve plate, square-hole sieve plate, circular-hole sieve plate, and grid-type sieve plate. The underlying reason for this result was that, for separation sieve plates of the same overall size, the separation area of the rectangular-hole sieve plate was larger than that of the other types. Although the grid-type sieve plate also exhibited a large separation area in the front view, a considerable amount of threshed material exits the threshing chamber at a certain angle relative to the sieve plate during separation, and the protruding structure of the grid-type sieve plate impeded the separation process. Therefore, among the different types of separation sieve plates, the rectangular-hole sieve plate achieved the lowest total threshing power consumption of 27.14 kW.

The effects of drum rotational speed on the threshing power consumption and mechanical efficiency of the threshing device are depicted in Fig. 8. The no-load power consumption of the threshing device exhibited a gradual upward trend with increasing drum rotational speed, rising from approximately 7.32 kW at 800 r/min to about 9.21 kW at 1000 r/min. This phenomenon was attributed to the increased mechanical losses, such as bearing friction and air resistance, at higher drum speeds, which elevated the basic energy consumption required to maintain the idling of the drum. The effective threshing power consumption of the device increased continuously with the rise in drum rotational speed, from approximately 17.76 kW at 800 r/min to around 20.68 kW at 1000 r/min. The increased rotational speed intensified the impact and kneading actions of the threshing components on the crop materials, thereby raising the effective energy consumption for threshing, with a growth rate slightly higher than that of the no-load power consumption. As the sum of the no-load power consumption and the effective threshing power consumption, the total threshing power consumption also presented a linear increasing trend with the elevation of drum speed, increasing from about 25.08 kW at 800 r/min to roughly 29.89 kW at 1000 r/min. The overall variation trend was steady without drastic fluctuations, demonstrating the stable operation of the device within the tested rotational speed range.

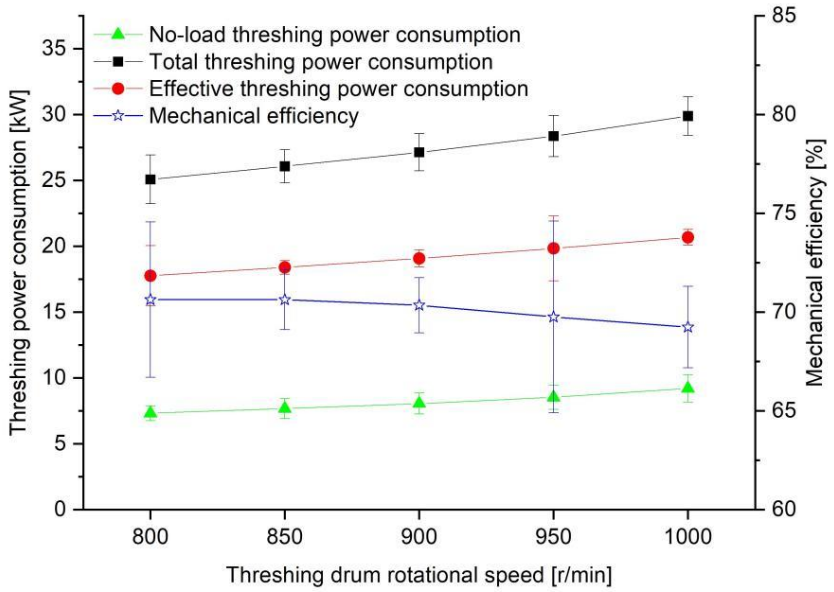

Fig. 8 - Effects of threshing-drum rotational speed on threshing power consumption and mechanical efficiency

As shown in Fig. 8, the mechanical efficiency of the threshing device remained relatively constant initially and then decreased as the drum rotational speed increased. Within the range of 800 ~ 900 r/min, the mechanical efficiency was stabilized at approximately 70.50%, indicating a high and stable energy utilization efficiency of the device in this speed interval. When the rotational speed exceeded 900 r/min, the mechanical efficiency began to decrease noticeably, dropping to about 69.76% at 950 r/min and further to 69.24% at 1000 r/min. The primary reason for the decline in mechanical efficiency was that the growth rate of no-load power consumption surpasses that of effective threshing power consumption at high speeds, with more energy dissipated in mechanical losses rather than being directly utilized for threshing operations, thus reducing the energy utilization efficiency.

The effects of deflector angle on the threshing power consumption and mechanical efficiency of the threshing device are illustrated in Fig. 9. The no-load power consumption remained basically stable at approximately 8.06 kW as the deflector angle increased from 50° to 70°.

This indicated that the variation in deflector angle exerted a negligible influence on mechanical losses during drum idling (such as bearing friction and air resistance), and the no-load power consumption was only determined by the inherent structure and operating state of the device. With the increase of the deflector angle, the effective threshing power consumption of the device exhibited a steady upward trend, rising gradually from approximately 18.68 kW at 50° to 19.60 kW at 70°. A larger deflector angle prolonged the residence time of crops in the threshing drum, promoted more uniform material distribution, and enhanced the interaction between threshing components and crops, thereby leading to a slight increase in effective threshing energy consumption. As the sum of no-load power consumption and effective threshing power consumption, the total threshing power consumption also increased slowly with the rise in deflector angle, from 26.74 kW at 50° to approximately 27.66 kW at 70°. The overall variation was gentle without obvious abrupt changes, demonstrating the stable operation of the device within the tested angle range.

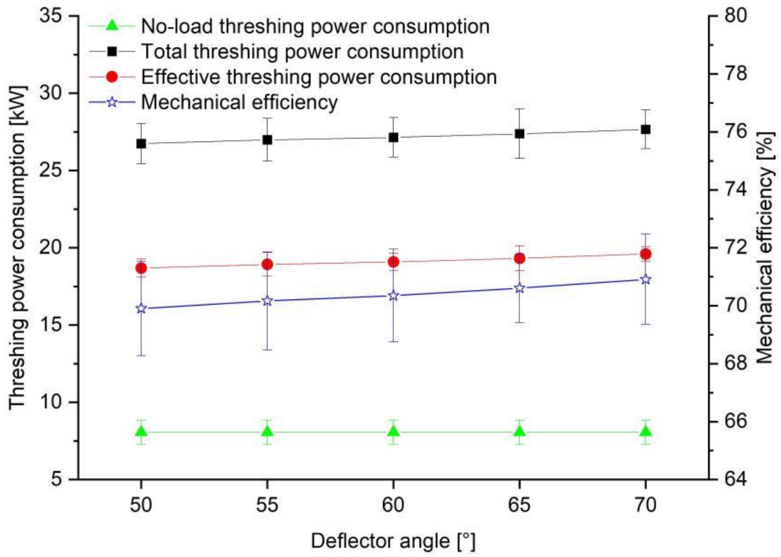

Fig. 9 - Effects of deflector angle on threshing power consumption and mechanical efficiency

As shown in Fig. 9, the mechanical efficiency of the threshing device displayed a continuous and steady upward trend with the increase in deflector angle, rising gradually from approximately 69.90% at 50° to about 70.91% at 70°. Although the increase amplitude was small, the trend was stable. The primary reason for the improved efficiency was that the growth rate of effective threshing power consumption was slightly higher than that of total power consumption, with more energy being efficiently utilized for threshing operations rather than mechanical losses, thus resulting in a slight optimization of energy utilization efficiency as the deflector angle increased.

The effects of concave sieve clearance on the threshing power consumption and mechanical efficiency of the threshing device are presented in Fig. 10. The no-load power consumption remained essentially constant at approximately 8.06 kW as the concave sieve clearance increased from 10 mm to 30 mm. This indicated that the adjustment of concave sieve clearance exerted no significant influence on the mechanical losses during drum idling, and the no-load power consumption was solely determined by the operating state of the device itself. The effective threshing power consumption of the device exhibited a gradual downward trend with the increase in concave sieve clearance, decreasing from 20.48 kW at 10 mm to 18.28 kW at 30 mm. A larger clearance weakened the squeezing and kneading interaction between the threshing components and the crop materials, and reduced the resistance of materials passing through the threshing zone, thereby lowering the effective energy consumption directly used for threshing operations. As the sum of the no-load power consumption and the effective power consumption, the total threshing power consumption also decreased steadily with the increase in clearance, from 28.54 kW at 10 mm to 26.34 kW at 30 mm. The overall variation was gentle without drastic fluctuations, indicating the stable operation of the device within the tested clearance range.

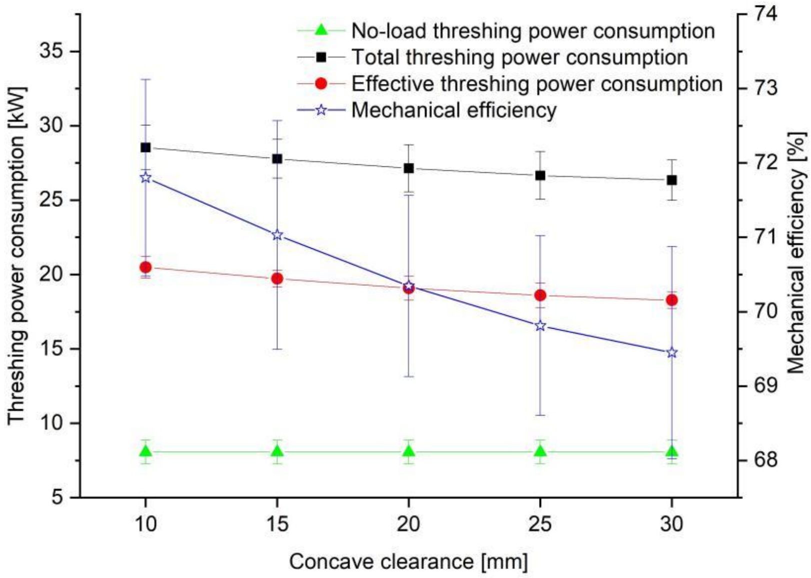

Fig. 10 - Effects of concave clearance on threshing power consumption and mechanical efficiency

As shown in Fig. 10, the mechanical efficiency of the threshing device decreased continuously as the concave clearance increased, declining from approximately 71.80% at 10 mm to 69.45% at 30 mm, a reduction of about 2.35 percentage points. This decrease occurred because effective threshing power consumption declined more rapidly than total power consumption. Consequently, a greater proportion of the total input power was associated with mechanical losses, such as those required to maintain drum rotation, rather than being used directly for threshing. Therefore, energy-use efficiency gradually decreased with increasing concave clearance.

The effects of feed rate on the threshing power consumption and mechanical efficiency of the device are illustrated in Fig. 11. Within the experimental range where the feed rate increased from 3.0 kg/s to 5.0 kg/s, the no-load power consumption remained stable at 8.06 kW without noticeable fluctuations. This indicated that the variation in feed rate exerted no significant influence on mechanical losses during drum idling. The no-load power consumption was determined only by the inherent structure and operating state of the device, independent of the working load, which conformed to the basic characteristics of the no-load power consumption of threshing devices. The effective threshing power consumption presented an approximately linear upward trend with the increase in feed rate, rising from about 13.98 kW at 3.0 kg/s to approximately 25.2 kW at 5.0 kg/s. The underlying reason was that a higher feed rate corresponded to a greater amount of crop material entering the threshing chamber per unit time, which synchronously enhanced the frequency and intensity of impact and kneading actions exerted by threshing components on the crop.

Consequently, the effective energy consumption directly employed for threshing operations increased substantially, with a stable growth rate and no obvious inflection point as the feed rate rose. As the sum of the no-load power consumption and the effective threshing power consumption, the total threshing power consumption exhibited a variation trend highly consistent with that of the effective threshing power consumption, increasing rapidly and approximately linearly from 22.04 kW at 3.0 kg/s to 33.26 kW at 5.0 kg/s. The continuous growth of total power consumption demonstrated that feed rate was a core sensitive factor affecting the overall energy consumption of the threshing device. The greater the operation load, the higher the energy consumption of the whole machine.

The mechanical efficiency of the threshing device increased continuously and rapidly with the rise in feed rate, from approximately 63.49% at 3.0 kg/s to 75.81% at 5.0 kg/s, with an increase of 12.32 percentage points, and the rising rate accelerated slightly with a higher feed rate. The essential reason was that the no-load power consumption remained constant. Meanwhile, the effective threshing power consumption increased linearly with feed rate. This led to a continuous rise in the proportion of effective threshing power consumption in total power consumption and a continuous decline in the proportion of mechanical losses. Therefore, energy utilization efficiency was significantly optimized. This regularity indicated that a proper increase in feed rate could considerably improve the energy utilization efficiency of threshing operations and reduce the energy consumption per unit grain mass. The premise was that the structural strength and threshing quality of the device were satisfied.

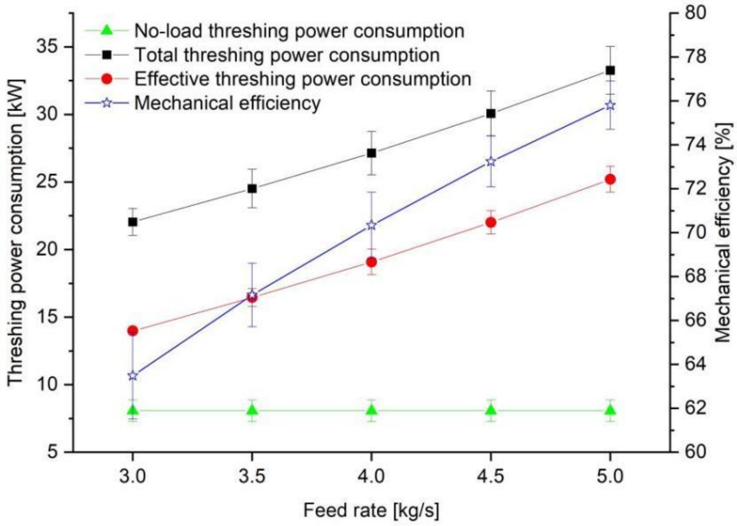

Fig. 11 - Effects of feed rate on threshing power consumption and mechanical efficiency

To further investigate the effects of operating parameters on the threshing power consumption of the device, the variation laws of these parameters on the threshing power consumption per unit feed rate of the threshing device were obtained, as shown in Fig. 12. The threshing power consumption per unit feed rate generally ranged from 4.4 kW/(kg/s) to 5.2 kW/(kg/s). It increased with the rise of drum rotational speed, deflector angle and feed rate, while decreasing with the increase of concave sieve clearance.

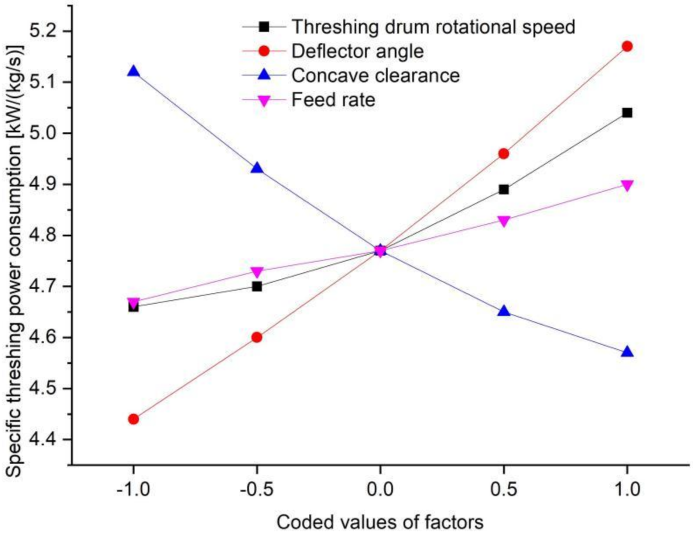

Fig. 12 - Effects of operating parameters on specific threshing power consumption

CONCLUSIONS

1) The effects of device structural parameters on the total threshing power consumption were clarified. Among the four modes of the threshing force adjustable concave sieve, the total threshing power consumption reached the minimum value of 27.14 kW when the threshing force adjustment plates were fully open, whereas the maximum value of 27.67 kW was obtained when the plates were fully closed. For different types of separation sieve plates on the upper part of the 360° separation device, the rectangular-hole sieve plate achieved the lowest total threshing power consumption of 27.14 kW.

2) Within the experimental range of drum rotational speed from 800 to 1000 r/min, with the increase of rotational speed, the no-load power consumption rose from 7.32 kW to 9.21 kW, the effective threshing power consumption increased from 17.76 kW to 20.68 kW, and the mechanical efficiency decreased from 70.63% to 69.24%. Within the deflector angle range of 50° to 70°, the no-load power consumption remained stable at 8.06 kW, the effective threshing power consumption increased from 18.68 kW to 19.60 kW, and the mechanical efficiency rose from 69.90% to 70.91%. Within the concave sieve clearance range of 10 to 30 mm, the no-load

power consumption was constant at 8.06 kW. The effective threshing power consumption decreased from 20.48 kW to 18.28 kW, and the mechanical efficiency dropped from 71.80% to 69.45%.

3) Within the feed rate range of 3.0 to 5.0 kg/s, with the increase of feed rate, the no-load power consumption remained stable at 8.06 kW, the effective threshing power consumption rose from 13.98 kW to 25.20 kW, and the mechanical efficiency increased from 63.49% to 75.81%. The threshing power consumption per unit feed rate of the device ranged from 4.4 kW/(kg/s) to 5.2 kW/(kg/s). It increased with the rise of drum rotational speed, deflector angle and feed rate, while decreasing with the increase of concave sieve clearance.

ACKNOWLEDGEMENT

This work was supported by Weifang City Science and Technology Development Plan Project (grant numbers 2025GX010) and the doctoral research start-up fee (grant numbers 44122025).

REFERENCES

[1] Ali K.A.M., Li C., Wang H., Mousa, A.M., Mohamed M.A.-E., (2024). Enhancing the performance of sunflower threshing machine through innovative enhancements, *Agriculture,* 14(2), 312, DOI: https://doi.org/10.3390/agriculture14020312

[2] Chen, L., Zhu, J., Liu, C., Zhang, C., Zhang, H., & Cai, Z., (2025). Optimal design and test of wheat plot breeding threshing device (小麦小区育种脱粒装置优化设计与试验), *Transactions of the Chinese Society for Agricultural Machinery*, 56(7), 72-81.

[3] Fan, C., Zhang, D., Li Y., Cui, T., He, X., Dong, J., & Zhao, H., (2022). Power consumption and performance of a maize thresher with automatic gap control based on feed rate monitoring, *Biosystems Engineering*, 216, 147-164.

[4] Jin, X., Zhu, X., Jin, C., & Cao, G., (2015). Research on the power consumption model of g rain threshing cylinder (谷物脱粒滚筒的功耗模型研究), *Journal of Chinese Agricultural Mechanization*, 36(3), 30-33+38.

[5] Jiang, T., Li, H., Huang, M., Zhang, M., Jin, M., & Guan, Z., (2025). Design and experiment of spiral Interlaced threshing cylinder for combine harvester (联合收获机螺旋交错排布式脱粒滚筒设计与试验), *Transactions of the Chinese Society for Agricultural Machinery*, 56(2), 314-324.

[6] Kiniulis V., Steponavičius D., Andriušis A., Kemzūraitė A., Jovarauskas D., (2017). Comparing performance of filler-plate-covered threshing cylinders. *Mechanics*, 23(5), 714-722.

[7] Li, Y., Tang, Z., Xu, L., Zhao, Z., & Li, H., (2011). Power analysis and experiment on longitudinal axial-threshing unit test- bed (纵轴流脱粒分离装置功耗分析与试验), *Transactions of the Chinese Society for Agricultural Machinery*, 42(6), 93-97.

[8] Liu, A., Xie, F., Zhu, L., Wang, X., Ji, B., & Kang, J., (2025). Design and experiment of adaptive threshing gap device for soybean combine harvester (大豆联合收获机脱粒间隙自适应装置设计与试验), *Journal of Chinese Agricultural Mechanization*, 56(12), 322-330+342.

[9] Lu, W., Zhang, D., (2012). Research on the power consumption model of threshing cylinder (谷物联合收获机脱粒滚筒功耗模型研究), *Journal of Agricultural Mechanization Research*, 34(12), 44-47.

[10] Mousaviraad M., Tekeste M.Z., (2020). Effect of grain moisture content on physical, mechanical, and bulk dynamic behaviour of maize. *Biosystems Engineering*, 195, pp. 186-197. DOI: https://doi.org/10.1016/j.biosystemseng.2020.04.012

[11] Qin, Y., Chen, M., Yang, T., Zhang, G., Jin, C., & Mo, G., (2025). Wheat harvesting quality online detection system and experimental verification, *INMATEH - Agricultural Engineering*, 76(2), 945-953.

[12] Ren, S., Xie, F., Luo, X., & Sun, S., (2013). Analysis and test of power consumption in paddy threshing using flexible and rigid teeth (柔性齿与刚性齿脱粒水稻功耗比较分析与试验), *Transactions of the Chinese Society of Agricultural Engineering*, 29(5), 12-18.

[13] Song, Z., Diao, P., Cui, P., Wei, M., Miao, H., & Yao, W., (2022). Design and experimental study of flexible threshing device for Longitudinal axial flow corn, *INMATEH - Agricultural Engineering*, 67(2), 155-165.

[14] Steponavičius D., Kemzūraitė A., Pužauskas E., Domeika R., Grigas A., Karalius D., (2023). Shape optimization of concave crossbars to increase threshing performance of moist corn ears. *Agriculture*, 13, pp. 983-1003. DOI: https://doi.org/10.3390/agriculture13050983

[15] Vlăduț N.-V., Biriș S.-Ș., Cârdei P., Găgeanu I., Cujbescu D., Ungureanu N., Popa L.-D., Perişoară L., Matei G., & Teliban G.-C., (2022). Contributions to the mathematical modeling of the threshing and

separation process in an axial flow combine, *Agriculture,* 12(10), 1520, DOI: https://doi.org/10.3390/agriculture12101520
[16] Vlăduț N.-V., Ungureanu N., Biriș S.-S., Voicea I., Nenciu F., Găgeanu I., Cujbescu D., Popa L.-D., Boruz S., Matei G., Ekielski A., Teliban G.-C., (2023). Research on the identification of some optimal threshing and separation regimes in the axial flow apparatus, *Agriculture*, 13(4): 838, DOI: https://doi.org/10.3390/agriculture13040838
[17] Wan, L., Yi, S., & Ma, Y., (2005). Study on power consumption of single axial flow threshing and separating unit of paddy (纵置单轴流滚筒脱粒与分离装置功耗性能试验研究), *J.of Heilongjiang August First Land Reclamation University*, 17(2), 56-58.
[18] Wang, W., Li, C., Chen, X., Liu, F., Wu, S., Qiao, X., Zhang, J., & Wang, B., (2025). Design and experiment of a threshing and separation system for a comb-type wheat plot harvester based on CFD-DEM, *INMATEH - Agricultural Engineering*, 77(3), 773-782.
[19] Waree, S., Somchai, C., & Khwantri, S., (2016). Design factors affecting losses and power consumption of an axial flow corn shelling unit, *Songklanakarin Journal of Science and Technology*, 38(5), 591-598.
[20] Xie, G., Zhang, G., Fu, J., Zhou, Y., Wang, Y., Gao, Y., Wang, W., & Mohamed, A., (2021). Comparing power consumption of drum and cylindrical rod-tooth longitudinal axial flow threshing roller (鼓形与圆柱形杆齿式纵轴流脱粒滚筒功耗对比试验), *Journal of Huazhong Agricultural University*. 40(1), 202-209.
[21] Xing, S., Cui, T., Zhang, D., Yang, L., He, X., Li, C., Dong, J., Jiang, Y., Wu, W., Zhang, C., & Du, Z., (2024). Design and optimization for a longitudinal-flow corn ear threshing device of low loss and low energy consumption, *Computers and Electronics in Agriculture*, 226, 1-16.
[22] Yu, Q., Yin, J., Cui, Y., Zha, Z., Guan, P., Wang, Y., Wang, X., & Geng, D., (2025). Study and experiment on a corn flexible threshing technology with single-point hinged structure based on DEM-MBD coupling, *INMATEH - Agricultural Engineering*, 76(2), 1190-1202.
[23] Zhang, J., Hu, J., Zhou, Z., Li, S., Liu, X., He, X., & Zhang, H., (2026). Design and experimental study of the rigid-flexible coupled structure for longitudinal axial-flow threshing device in high-moisture corn (高含水率玉米纵轴流脱粒装置刚柔耦合结构设计与试验), *Transactions of the Chinese Society of Agricultural Engineering*, 42(1), 58-70.
[24] Zhang, M., Wu, C., Lu, Y., Yu, S., & Yu, X., (2010). Experimental study of power consumption on threshing and separating of canola indirect harvest (油菜分段收获脱粒分离功率消耗试验研究), *Journal of China Agricultural University*, 15(4), 120-123.
[25] Zhou, X., Wang, Z., Tian, L., Su, Z., & Ding, Z., (2022). Innovative design and performance test of threshing-separating device for horizontal axial-flow combine harvester, *INMATEH - Agricultural Engineering*, 67(2), 497-508.